Exploring Chromodomain Genes in the Fungus *Fusarium graminearum* Through Targeted Genetic Manipulation

by

Alec J. Peters

A PROJECT

Submitted to

Oregon State University

in partial fulfillment of
the requirements for the
degree of

Honors Baccalaureate of Science in Bioresource Research,

Biotechnology, Genomics/Bioinformatics

APPROVED:

Michael Freitag, Biochemistry and Biophysics Date

David Hendrix, Biochemistry and Biophysics Date

Lanelle Conolly, Biochemistry and Biophysics Date

Katharine G. Field, BRR Director Date

I understand that my project will become part of the permanent collection of the Oregon State University Library, and will become part of the Scholars Archive collection for BioResource Research. My signature below authorizes release of my project and thesis to any reader upon request.

Alec J. Peters, Author Date

Exploring Chromodomain Genes in the Fungus *Fusarium graminearum* Through Targeted Genetic Manipulation

ABSTRACT

DNA segments in the fungus *Fusarium graminearum* were identified as possible genes encoding for chromodomain proteins (CDPs), and targeted for genetic manipulation. Targeted single-gene deletion strains, as wells as GFP-S tag fusion strains, were generated from wildtype *F. graminearum* protoplasts, and verified strains were screened for phenotypic differences, such as changes in growth, appearance, and levels of certain histone marks in the genome. It was found that the *FgCdp6* gene is required for normal growth and appearance of *F. graminearum*, and its protein product localizes to nuclei of asexual spores. Further studies including western blots suggested that the CDP encoded by the *FgCdp6* gene is a homolog of the yeast protein Eaf3, which is involved in both histone acetylation and deacetylation complexes.

INTRODUCTION

All of the information that a typical cell requires to live, grow, respond to different stimuli, and reproduce can be found in the nucleus in the form of DNA. Genes, segments of DNA that are known to hold the information to create a certain product such as a protein, are transcribed into mRNA, which is then transported out of the nucleus and translated into a protein product. The various proteins that are created in this way during a mature cell's life carry out all of the required processes for life such as metabolizing high-energy substances to synthesize ATP, maintaining cellular shape, and reproduction via mitosis.

The expression of a gene, transcription and translation of that gene into its cellular product, can change over the course of a cell's lifespan. While some genes are expressed throughout a cell's lifespan, certain genes are only expressed as a cell is developing, such as when a group of stem cells combine and develop into a single, multinucleated muscle fiber. Other genes are only expressed in response to certain stimuli, such as when *Escherichia coli* cells in the presence of allolactose express the *lac* operon to produce the enzymes required to metabolize lactose [1].

There are cellular processes that regulate and control gene expression, and the study of these processes that do not actively change the DNA sequence is referred to as epigenetics [2].

Nuclear DNA is almost never found simply as DNA; it is in fact complexed with other proteins and sometimes RNA, collectively known as "chromatin". The basic repeating unit of chromatin is called the nucleosome, and consists of DNA wrapped around octameric protein complexes made of histones. This arrangement of a long strand of DNA wrapping around many individual histone octamers is often compared to "beads on a string" [3].

The arrangement of chromatin can change, and the nucleosomes of chromatin can be either densely packed together, making "heterochromatin", or loosely packed to make "euchromatin." The DNA in euchromatin is accessible to cellular complexes involved in transcription, and genes in euchromatin can be actively expressed and are therefore active [4]. DNA found in heterochromatic regions cannot be accessed by the transcriptional machinery of the cell, and these genes are not expressed, or silent [4,5].

Chemical modifications of the amino acids composing the tails of histones has been found to influence the arrangement of chromatin and the expression of genes [6]. Examples of the different chemical modifications made to histone tail include adding a methyl group or acetyl group to certain amino acids. Both the type of the chemical modification as well as the position of the modified amino acid influence chromatin packing and gene expression. For example, the trimethylation of lysine 4 on histone 3 (H3K4me3) has been observed to induce euchromatin formation and gene activation, while the trimethylation of lysine 27 on the same histone (H3K27me3) has been observed to induce heterochromatin formation and gene silencing [7,8]. These different modifications on different histone tail residues are known as histone marks.

Two major steps exist for the proper regulation of gene expression through histone modification. The first is the accurate modification of histone tail residues, and second is the "reading," or binding to the histone modification, of a mark that ultimately leads to a cell response and chromatin structural regulation. For a protein or protein complex to carry out either of these functions, it must have a domain that recognizes histone modifications. This protein domain has been termed the chromatin organization modifier domain, or chromodomain [9].

The chromodomain was originally identified in *Drosophila melanogaster*, as a 30 amino acid residue protein domain involved in two different complexes that regulate histone modification, the Polycomb (Pc) and HP1 complexes [9]. These chromodomain protein (CDP) complexes and others have had their cellular functions elucidated and also have been found to be conserved across many species, including mammals [10,11]. For example, the Polycomb Repressive Complex 2 (PRC2) is a protein complex containing a CDP, KMT6 in fungi and EZH2 in humans, that is involved in the trimethylation of histone H3 lysine 27 (H3K27me3), a silencing histone modification, while the HP1 complex, also containing a CDP, has been found to regulate histone H3 lysine 9 methylation (H3K9me), another silencing histone mark [10,11].

As more and more proteins containing domains similar to the Pc and HP1 chomodomains were discovered to bind chromatin, the motif was expanded to include about 50 residues [9]. More CDP homologs have been found in a variety of organisms, and these have had their functions elucidated as well. For example, the conserved NuA4 complex has been found to regulate histone acetylation on both histones H3 and H4 [12].

Fusarium graminearum is a filamentous fungus that has been associated with diseases of cereal plants, especially Fusarium Head Blight (FHB) on wheat. FHB causes hundreds of millions of dollars every year in damages to crop yields, and toxins found in contaminated foods can be

very harmful to individuals who consume them [9]. Exploring gene expression in *F. graminearum* could yield insights that lead to the development of compounds that combat FHB infection, either by killing the fungus or reducing the expression of harmful toxins.

F. graminearum has also been found to contain a large amount of a certain epigenetic mark not found in some other fungi (such as yeasts), H3K27me3, which is generated by the PRC2 complex and read by the PRC 1 complex in humans and flies [10]. This provides an opportunity to study the regulation of this mark in a genetically tractable eukaryote to determine if H3K27me3 is regulated in a similar fashion as in humans and to advance mechanistic studies at a quicker pace. There is evidence that suggests there is no true PRC1 complex in *F. graminearum,* so it is suspected that other CDPs regulate H3K27me3 in the fungus. The genome of *F. graminearum* has been sequenced, and genes that could code for chromodomain proteins were selected for targeted genetic manipulation.

Gene candidates that had the most potential to code for a functional CDP were selected based on sequence homology with functional genes in other species, such as *D. melanogaster* and *Neurospora crassa* (Table 1). Two of the genes were found to code for homologs of the proteins HP1 and CHD1 (a chromatin remodeling factor), the other eight do not have their functions elucidated and were selected for study through targeted genetic manipulation [13]. The four most promising gene candidates based on sequence homology were *FgCdp1, FgCdp2, FgCdp3,* and *FgCdp6. FgCdp1* is suspected to be involved in centromere histone modification, while *FgCdp3* has a rather unclear cellular function. *FgCdp2* is suspected to be a homolog of the *N. crassa* gene coding for CDP2, which is involved in a HP1 complex regulating H3K9me [11]. *FgCdp6* is thought to code for a protein with a MRG (MORF4 related gene) motif, a chromodomain first found in MORF4 (mortality factor on chromosome 4), a gene involved in cellular aging; FgCDP6

may be involved in histone acetylation [14]. Others, such as *FgCdp5*, could be species-specific CDP genes not found in close relatives such as *N. crassa*.

To study these CDP gene candidates, gene deletion strains in which one of these CDP genes is absent, as well as fusion genes in which one of the CDP genes was fused with green fluorescent protein (GFP) and an S tag that helps in protein purification [15], were synthesized and verified for targeted DNA insertion by Southern blotting. Gene deletion strains were compared to the wild type fungus to look for any obvious phenotypic differences such as appearance, growth rate, fertility during selfing, and fluorescent localizations *in vivo* (for GFP tagged strains).

Any gene candidates that were identified as coding for functional genes involved in cellular processes, demonstrated with obvious phenotypic differences between wildtype and verified deletion strains, were further studied to assess the functions of the protein products in epigenetic regulation. Western blot analyses identified changes in histone marks between wildtype and deletion strains.

METHODS

Media and Conditions for *F. graminearum* Growth

F. graminearum strains were grown in either yeast extract-peptone-dextrose (YPD) to generate vegetative tissue, or carboxymethylcellulose (CMC) to generate asexual spores. Both fungal vegetative tissue and macroconidia were grown, collected, and stored as described in [8]. Selfing of strains was set up on carrot agar [8].

Synthesis of DNA Cassettes

DNA cassettes intended to replace specific CDP genes were synthesized through two rounds of fusion PCR. A cassette conferring resistance to the antibiotic neomycin/G418 (*neo*$^{+}$*)* was synthesized from the plasmid pLC12_pzeroneo with the oligonucleotide primers loxPF and loxPR (OMF 1959, 5'-ACAAGTAAGAATTCGATATCAAGCTTATC-3', and OMF 1958, 5'-CGAGCTCGGATCCATAACTTCGTATAGCA-3', respectively) using fusion PCR [8]. One kilobase (kb) DNA segments flanking the targeted CDP candidate gene on both the 5' and 3' sides were synthesized from wildtype *F. graminearum* (PH-1, or FMF1) genomic DNA using primers specific to the candidate genes (Table 2).

These 5'- and 3'-flanking segments were fused to the *neo*$^{+}$ cassette in another PCR reaction that first generated these fused fragments, and then amplified them with *neo* split marker primers (neo_SM_F, OMF 600, 5'-AGGCGATGCGCTGCGAATCGG -3', and neo_SM_R, OMF 601, 5'-TTGAACAAGATGGATTGCACG-3') and candidate specific primers (Table 3) [17].

Cassettes intended to fuse targeted CDP candidate genes with the gene encoding green fluorescent protein (GFP), an S tag that helps in protein isolation and purification, and a gene conferring resistance to the antibiotic hygromycin (*hph*$^{+}$) were created in the same two-step manner [8,15,17]. The GFP-S tag-*hph*$^{+}$ cassette was generated by fusion PCR using the plasmid pZero_NcGFP_Stag and the primers OMF 1762 (5'-GGCGGAGGCGGCGGAGGCGGAGGCGGAGG-3') and OMF 1958, and candidate-specific 5' and 3' flanking regions were fused with this fragment as above, except that the 5' flanking fragment was the first 1kb of DNA 5' to the site of fusion with the GFP-S tag-*hph*$^{+}$ fragment (Table 4). This site of fusion is at the end of the gene candidates, right before the stop codon.

The 5' and 3' flanking DNA segments were fused with the GFP-S tag-*hph*$^{+}$ cassette using either the hph_SM_R primer (OMF 3228, 5'- TCGCCTCGCTCCAGTCAATGACC-3') or the hph_SM_F primer (OMF 3227, 5' - AAAAAGCCTGAACTCACCGCGACG -3') in place of the neo split marker primers (Table 5) [8,17]. All PCR fragments were gel-purified using the Qiagen Qiaquick gel purification kit (Valencia, CA) [8].

Protoplasting and Transforming PH-1

PH-1 protoplasts were generated from mycelia, and either *neo*$^{+}$ deletion or GFP-S tag-*hph*$^{+}$ fusion cassettes were transformed into protoplasts as described elsewhere [8]. Resistant transformant colonies were picked and strains were screened for targeted gene replacements or fusions by PCR and Southern blot analyses [8].

Southern Blot Analyses

Both gene deletion strains and GFP-S tag fusion strains had genomic DNA isolated as described [18]. Genomic DNA (gDNA) of gene deletion strains of *FgCdp1*, or Δ*FgCdp1::neo* strains, were digested with the restriction enzymes *Xho*I and *Pvu*II. gDNA of *FgCdp1* GFP fusion strains, or *FgCdp1-GFP-S tag-hph* strains, were digested with *Sal*I. gDNA of Δ*FgCdp2::neo* strains were digested with *Xho*I and *Kpn*I, while gDNA of *FgCdp2-GFP-S tag-hph* strains were digested with the enzyme *Sma*I. gDNA of Δ*FgCdp3::neo* strains were digested with *Xho*I and *Kpn*I, and gDNA of *FgCdp3-GFP-S tag-hph* strains were digested with *Nae*I. Δ*FgCdp5::neo*, Δ*FgCdp9::neo*, and Δ*FgChd3::neo* were digested with *Hind*III, *Kpn*I, and *Age*I and *Dra*I, respectively. The enzymes *Bgl*II and *Mlu*I were used to digest gDNA of both Δ*FgCdp6::neo* and *FgCdp6-GFP-S tag-hph* strains. Southern blots were performed as described [19].

Screening for Phenotypic Differences

Transformant strains verified by Southern blot analysis were compared to PH-1 to observe any differences in appearance. Self-crosses were set up on carrot agar to determine if strains would produce structures associated with fertility, as well as ascospores [8].

To assay differences in linear growth between wildtype PH-1 and deletion strains, conidia (asexual spores) of each strain and PH-1 were grown in 50ml CMC shaking at 200rpm at room temperature (RT, about 26° C) for four days. Conidia were harvested by filtration through cheesecloth, and quantified using a hemocytometer. 2000 conidia were spread on an YPD agar plate to isolate single spores. Single spores were inoculated on one end of an YPD agar plate, and every day linear growth of the fungus to the other end of the plate (in cm) was marked and recorded. Multiple plates were used for growth determination of each strain, and growth rates were determined on both rich (YPD) and minimal nutrient (FMM, *Fusarium* minimal medium) agar plates [8].

Western Blot Analyses

Histones were extracted from vegetative tissue grown in YPD, and Western blot analyses were conducted as described elsewhere [8]. Four primary antibodies used were derived from rabbit immune cells and detect H3K4me2, overall acetylation of histone H3, acetylation of histone H3 lysine 27 (H3K27Ac), and trimethylation of histone H3 lysine 36 (H3K36me3). The secondary antibody used was derived from goat immune cells and is specific for rabbit antibodies.

RESULTS

Verification of Transformant Strains by Southern Blotting

Not all transformations yielded colonies. The GFP fusion transformations for *FgCdp5*, *FgCdp8*, *FgCdp9*, and *FgChd3* did not produce any transformant colonies, likely due to unsuccessful transformations. However, the transformations to generate deletion strains were successful for seven of eight candidate genes, and the GFP fusion transformations were successful for *FgCdp1*, *FgCdp2*, *FgCdp3*, and *FgCdp6*. Colonies were picked, selected on appropriate antibiotic YPD agar, and screened for targeted gene insertion.

The Southern blots for *ΔFgCdp1::neo* deletion strains are shown in Figure 1. When probed with a fragment specifying the gene, expected fragment size for the wild type was 5.3 kb, and deletion strains are expected to have no bound probe (empty lanes). When using the *neo*$^+$ probe, the wildtype lane was expected to have no fragments, and the transformants were expected to have two fragments at 2.8 and 3.4 kb. GFP fusion strains were expected to have a fragment size of 5.2 kb while the wildtype was expected to have a band at approximately 2.7 kb when using the gene probe (Figure 2). The GFP fusion strains were expected to have the same size band when using an *hph*$^+$ probe, while the wildtype was expected to have no probe binding. Blots for *ΔFgCdp2::neo* deletion strains are shown in Figure 3. The expected size for the wildtype DNA fragments was 4.0 kb using the *FgCdp2* gene probe, and 0 kb (no signal detected) using the *neo*$^+$ probe. Expected sizes for transformant strains were no expected band using the gene probe and 4.5 kb using the *neo*$^+$ probe. GFP fusion strains had an expected size of 5.7 kb using the gene probe, while the wildtype had an expected fragment size of 3.3 kb (Figure 4). Using an *hph*$^+$ probe, the expected size for GFP fusion strains was 5.7 kb, and there was no expected band for the wildtype DNA. Southern blot results for *ΔFgCdp3::neo* deletion strains are shown in Figure 5.

The expected size of the wildtype DNA probed with the *FgCdp3* gene was 1.2 kb, and no band was expected when probed with *neo*$^+$ probe (Fig. 5). Expected transformant DNA fragment sizes were 3.4 kb using the *neo*$^+$ probe, and no band was expected when using the gene probe. For *FgCdp3-GFP-S tag-hph*$^+$ strains, expected sizes when probed with the gene was 9.3 kb, and 6.9 kb for wildtype (Figure 6). The expected fragment size when probed with *hph*$^+$ was 9.3 kb for GFP tagged strains, and no bad was expected for wildtype. *ΔFgCdp5::neo* deletion strain Southern blot results are shown in Figure 7, *ΔFgCdp9::neo* deletion results are shown in Figure 8, and *ΔFgChd3::neo* Southern results are in Figure 9. For *ΔFgCdp5::neo*, the expected size for the wild type was 5.0 kb (no band was expected for the deletion strain). For *ΔFgCdp9::neo*, expected sizes for the wildtype were 3.7 kb when probing with the gene and no expected bands when probing with *neo*$^+$. Expected sizes for the deletion strain were 3.7 kb when probing with *neo*$^+$ and no expected bands when probing with the gene. For *ΔFgChd3::neo*, expected sizes for the wildtype were 8.4 kb when probing with the gene and no expected bands when probing with *neo*$^+$, and expected sizes for the deletion strain were 4.8 kb when probing with *neo*$^+$ and no expected bands when probing with the gene. Southern blot results for both *ΔFgCdp6::neo* deletion strains as well as *FgCdp6-GFP-S tag-hph*$^+$ strains are shown in Figures 10 and 11. Expected sizes wildtype lanes were 5.4 kb using the *FgCdp6* gene probe and no expected bands using either the *neo*$^+$ or *hph*$^+$ probe. Deletion strains were expected to have no fragments when using the gene probe and a fragment size of 5.0 kb using the *neo*$^+$ probe. GFP tagged strains were expected to have a size of 7.9 kb when using either the gene probe or the *hph*$^+$ probe.

Screening for Phenotypic Differences

Southern blot verified strains were screened for phenotypic differences. Most strains, except for ones in which *FgCdp6* was successfully manipulated, exhibited the same phenotype as wildtype PH-1 (Figure 12). Both *ΔFgCdp6::neo* deletion strains as well as *FgCdp6-GFP-S tag-hph*$^{+}$ fusion strains had altered phenotypes from wildtype, with a change in appearance as well as growth rate (Figure 13). The difference in growth rate was measured for the deletion strain (Figure 14). Conidia of GFP tagged strains were examined under a fluorescent microscope to observe any signs of GFP localization in the nucleus, which is seen only in the tagged *FgCdp6* strain (Figure 15). Verified transformant strains, with their corresponding lanes on respective Southern blots, are displayed in Table 6.

Western Blotting

Western blot analyses were conducted to observe changes in histone marks between wildtype and *FgCdp6* deleted strains (Figure 16). Coomassie staining suggested that the same relative amount of histones was loaded in each lane in the blotted gels, so the blots could be used as a rough estimate of the change in histone marks in the genome due to the removal of the *FgCdp6* gene.

On western blots, the calf thymus control did not show a signal when treated with H3 acetyl- or H3K27ac- specific antibodies. Relative amounts of signal were equal between wiltdype and *ΔFgCdp6::neo* deletion strains when using H3K4me2-, H3 acetyl-, or H3K27ac- specific antibodies. There was an apparent decrease in the levels of H3K36me3 between wildtype and *ΔFgCdp6::neo* deletion strains.

DISCUSSION

Transformant colonies that were picked and selected onto antibiotic containing agar were found to not contain a targeted gene insertion. This is likely due to successful transformation of the DNA cassette containing the antibiotic resistance gene into the genome at a different locus or insertion right next to the targeted locus. Both of these events would lead to transformant colonies that contained a wildtype copy of the gene of interest as well as the antibiotic resistance gene.

Some Southern blots had bands that were not expected or had sizes different than expected for wildtype gDNA, such as the blots in Figures 1 and 5. This is likely due to either the binding of the probe DNA at a locus other than the one of interest, or non-specific restriction enzyme digestion. In both blots where this was the case (Figures 1 and 5), deletion strains were verified by and absence of signals found in in wildtype control when using a gene-specific probe. Numbers of verified strains obtained from the transformations are displayed in Table 6.

A few transformations, such as ones to remove *FgCdp8*, did not yield any transformant colonies with the gene removed (the few transformants picked contained both the gene and the antibiotic resistance gene intended to be the replacement). This could indicate that complete removal of the gene from the *F. graminearum* genome results in a lethal phenotype, or that the transformation was unsuccessful. Further studies, such as successful deletions or fusion of these genes with GFP, could yield more information on whether they are pseudogenes or if they are required for survival.

The strains that did have targeted gene insertions were used to examine phenotypic differences. All strains except for those involving *FgCdp6* exhibited the same phenotype as wildtype *F. graminearum*. This indicates that these gene candidates could be pseudogenes that have high sequence homology with genes but are not transcribed and do not code for a functional

protein. Alternatively, the gene candidates could be functional genes that could code for a protein with a redundant function in the organism that, when removed, does not hinder the organism in any way. Further studies are needed before gene candidates can be identified as pseudogenes. One possible experiment would be to create a strain with all of the CDP candidate genes deleted, and selectively reintroduce individual genes to identify which ones restore the phenotype to that of PH-1.

Deletion strains of *FgCdp6* exhibited a marked difference in phenotype from the wildtype, including a significant reduction in growth rate (Figure 14) and an obvious difference in appearance. The *FgCdp6-GFP* strain also exhibited this phenotype, however it was not as pronounced as the deletion strains. Asexual spores of an *FgCdp6* GFP tagged strain showed fluorescent localization to the nuclei of cells, which is an indication of a chromodomain protein [20]. These observations provide evidence that the *FgCdp6* gene candidate is a functional gene coding for a CDP necessary for normal growth in *F. graminearum*. GFP tagged versions of the CDP6 gene seem to retain limited function, giving the *FgCdp6-GFP* strain a phenotype that was not as pronounced as the deletion strains with none of the protein at all.

Spores of GFP tagged strains other than those of *FgCdp6* showed no fluorescent localization to any specific cellular compartment, which indicates these CDP gene candidates either do not code for CDPs, or that their protein products are so few in number that there is no significant difference in fluorescence between them and the background fluorescence. These results were interesting especially for *FgCdp1* and *FgCdp2*, which have been shown to be localized to the nucleus in other organisms [11]. It is possible that these proteins are not abundant enough in *F. graminearum* to show signs of localization under a fluorescent microscope, these proteins

are nonfunctional in this fungus, or adding a C-terminal GFP interferes with the function of the proteins, in which case they would not localize in cells.

The DNA sequence of *FgCdp6* indicated that it is a possible homolog of the *EAF3* gene in yeast, a CDP that is part of the NuA4 histone acetyltransferase complex responsible for acetylation of amino acid residues on both histones H3 and H4 [21]. This suggests that *FgCdp6* is involved in histone acetylation, which is thought to be a transcriptional activation mark. Removing this gene from the genome would reduce transcriptional activation of genes, including some that function in normal growth, and helps to explain the reduction in growth rate observed in *FgCdp6* gene deletion strains.

In Western blots H3K4me2 was used as a negative control (i.e. no change in signal was expected between strains), and did not show any signs of change between wildtype and an *FgCdp6* deletion strain. Other western blots indicated that there is no global change in patterns of histone three acetylation, nor in H3K27ac. This was expected, for the absence of the Eaf3 protein in yeast did not change the overall levels of histone acetylation, but instead changed the patterns of acetylation within the genome itself [22]. No signal, indicating no antibody binding, was seen in the calf thymus histone positive control lanes when using either the H3 acetylation or H3K27ac antibodies. This could have been because there was none of these marks in the calf thymus histones (which is unlikely), the antibody was not specific to the calf thymus histones, or that the antibody did not bind as expected. Repeating western blots to look for the same patterns would help show that the acquired results are credible.

An apparent decrease in the levels of H3K36me3 was observed when the *FgCdp6* gene was removed from the *F. graminearum* genome. As well as being a component of the NuA4 histone acetylase complex [22,23], Eaf3 has been found to be involved in the reading of

H3K36me3 and subsequent recruitment of the histone deacetylase complex Rpd3S [24,25] (Table 7). Observing a decrease in H3K36me3 levels indicates that the *FgCdp6* gene codes for a protein involved in the regulation of histones using H3K36me3. It is likely that the *FgCdp6* gene encodes a homolog of Eaf3 and is thus involved in similar processes as Eaf3 would be, albeit maybe in a different way.

There has been no indication of a change in genomic H3K36me3 levels in other studies of the Eaf3 protein, which was observed when western blotting. This could indicate that either the CDP6 protein in *F. graminearum* is related to the Eaf3 protein but has a different function altogether, the Eaf3 protein in *F. graminearum* has an extra function in regulating H3K36me3 levels, or that regulation of H3K36me3 is a previously unknown function of Eaf3.

Further studies of the *FgCdp6* gene and its protein product will yield more information on the function of this gene in *F. graminearum*. To further confirm that the removal of the *FgCdp6* gene resulted in the pronounced phenotypic difference, a genetic reinsertion of the gene will be conducted on the deletion strain. It would be expected that the reintroduction of the gene would result in a reversion to the wildtype phenotype.

The GFP-S tag fusion strain can be used for complex isolation/pull-down and analysis through mass spectrometry. This would determine the sizes and possible identities of proteins in complexes with the FgCdp6 CDP. This CDP encoded by *FgCdp6* would be more likely to be a homolog of Eaf3 if it is found to be in complexes similar to the NuA4 acetylase and Rpd3S histone deacetylase in *F. graminearum* (Table 7). Chromatin immunoprecipitation followed by high-throughput sequencing would identify which genes are influenced by this protein. Ultimately, the function of the *FgCdp6* gene and its protein product in *F. graminearum* will be elucidated, helping further the understanding of the mechanisms of epigenetic regulation of genes.

TABLES AND FIGURES

Table 1: CDP gene candidates in *Fusarium graminearum*

CDP Gene Candidate	*Fusarium* Gene ID	*N. crassa* Homologous Gene ID	Proposed Function
FgCdp1	FGSG_01512	NCU08362	Centromere Regulation
FgCdp2	FGSG_05030	NCU00738	H3K9me Regulation
FgCdp3	FGSG_04328	NCU01522	Unclear Function
FgCdp5	FGSG_11309	N/A	Unclear Function
FgCdp6	FGSG_14036	NCU06788/NCU06787*	Histone Acetylation
FgCdp8	FGSG_03473	N/A	Unclear Function
FgCdp9	FGSG_02144	N/A	Unclear Function
FcChd3	FGSG_07346	NCU06696	Histone Deacetylation
HP1	FGSG_08763	NCU04017	H3K9me, Silencing
CHD1	FGSG_07102	NCU03060	Chromatin Remodeling

*Gene is split in *N. crassa*

Table 2: Primers for 5' and 3' flanking regions of CDP candidate gene deletion cassettes

Gene Candidate	Fragment	Primer*	Sequence (5' to 3')
FgCdp1	5' Flank	OMF 2960	AGACCCGGGGCCAACCTTGACGTAGGATCG
		OMF 2965	GATAAGCTTGATATCGAATTCTTACTTGTCTTGCTGAATGGCAAAGGCAA
	3' Flank	OMF 2963	TGCTATACGAAGTTATGGATCCGAGCTCGGGTGGGAGAGAGTCTATTTGG
		OMF 2964	TGACCAATCGGCCTCGAACCG
FgCdp2	5' Flank	OMF 2970	GCGGGATCCGATTGAAGAATGTCGTTGTGC
		OMF 2971	GATAAGCTTGATATCGAATTCTTACTTGTCCTCAGTGTTTGCGAATTCCC
	3' Flank	OMF 2968	TGCTATACGAAGTTATGGATCCGAGCTCGGAGTTTGGATAAGCGGAGGCC
		OMF 2969	TCCGGGCATTCTATGAGTACG
FgCdp3	5' Flank	OMF 2977	GCCTCTAGATGGCGGGACATAAGGGCTACC
		OMF 2978	GATAAGCTTGATATCGAATTCTTACTTGTGGTTGAGATGATGCAGTTGGC
	3' Flank	OMF 2975	TGCTATACGAAGTTATGGATCCGAGCTCGGACACGATGGTTGGAGTTACAG
		OMF 2976	TACTAACAGCCATAGTCATCC
FgCdp5	5' Flank	OMF 3044	TCTTCAACAGCGCTGGCTTGC
		OMF 3045	GATAAGCTTGATATCGAATTCTTACTTGTTAGCCCTGTGACGAGAGAAGA
	3' Flank	OMF 3047	TGCTATACGAAGTTATGGATCCGAGCTCGGACTGATGAGACACGTGCGAA
		OMF 3048	CAGAGCCACGATACAGTGTCGC
FgCdp6	5' Flank	OMF 2984	GCCGAATTCAAAGTGTTCAATGATACTGCC
		OMF 2985	GATAAGCTTGATATCGAATTCTTACTTGTGATGATGATGGTTGTGGTTGTG
	3' Flank	OMF 2982	TGCTATACGAAGTTATGGATCCGAGCTCGATTCAGCCAACCGATCCTTGATC
		OMF 2983	TATCATGAGTTAAACTTCAAG
FgCdp8	5' Flank	OMF 3054	GAGGTGAGCAGTAACAAAGCG
		OMF 3055	GATAAGCTTGATATCGAATTCTTACTTGTGATGTGTTGGTGGTAATCAAG
	3' Flank	OMF 3057	TGCTATACGAAGTTATGGATCCGAGCTCGGGCGGGGAAATCTTTGCAGGC
		OMF 3058	AGCTTATCGATTTCGGATTCG
FgCdp9	5' Flank	OMF 3059	ACATTCGAGCTATAGACATGG
		OMF 3060	GATAAGCTTGATATCGAATTCTTACTTGTGGCGTCTCGAGTCATTGGGGG
	3' Flank	OMF 3062	TGCTATACGAAGTTATGGATCCGAGCTCGCGGATGGCGCGCATGTAGACG
		OMF 3063	CGTTGCTAATTGGCATGACAGG
FgChd3	5' Flank	OMF 3032	GTCGGAAAGACCGTGGCTGAA
		OMF 3033	GATAAGCTTGATATCGAATTCTTACTTGTTTATGCTGGTGCGATCAAGTG
	3' Flank	OMF 3036	TGCTATACGAAGTTATGGATCCGAGCTCGCCTGGGTCGGCCTGCGCAAGC
		OMF 3037	CGTGGTGCTGATGTCTGATAGG

*Primers are listed as pairs, first the forward then the reverse.

Table 3: Primers used to construct *neo*$^{+}$ deletion cassettes

Gene Candidate	Fragment	Primer	Gene Candidate	Fragment	Primer
FgCdp1	5' Flank	OMF 2960	*FgCdp6*	5' Flank	OMF 2984
		OMF 601			OMF 601
	3' Flank	OMF 600		3' Flank	OMF 600
		OMF 2964			OMF 2983
FgCdp2	5' Flank	OMF 2970	*FgCdp8*	5' Flank	OMF 3054
		OMF 601			OMF 601
	3' Flank	OMF 600		3' Flank	OMF 600
		OMF 2969			OMF 3068
FgCdp3	5' Flank	OMF 2977	*FgCdp9*	5' Flank	OMF 3059
		OMF 601			OMF 601
	3' Flank	OMF 600		3' Flank	OMF 600
		OMF 2976			OMF 3063
FgCdp5	5' Flank	OMF 3044	*FgChd3*	5' Flank	OMF 3032
		OMF 601			OMF 601
	3' Flank	OMF 600		3' Flank	OMF 600
		OMF 3048			OMF 3037

Table 4: Primers used to amplify 5' flanks in GFP-S tag-*hph*$^{+}$ fusion cassettes

Gene Candidate	Primer	Sequence (5' to 3')
FgCdp1	OMF 2961	GCCTCTAGACTGGTTTAATATGAATCATGG
	OMF 2962	CCTCCGCCTCCGCCTCCGCCGCCTCCGCCGTGCTTCATTTCGAAATCCCG
FgCdp2	OMF 2970	GCGGGATCCGATTGAAGAATGTCGTTGTGC
	OMF 2967	CCTCCGCCTCCGCCTCCGCCGCCTCCGCCGAGATCTAATCCGTTTCCAACC
FgCdp3	OMF 2973	AGACGTCGAGCGAATCGAAGC
	OMF 2974	CCTCCGCCTCCGCCTCCGCCGCCTCCGCCTCTGACATCACGTCGAACCTC
FgCdp5	OMF 3044	TCTTCAACAGCGCTGGCTTGC
	OMF 3046	CCTCCGCCTCCGCCTCCGCCGCCTCCGCCCTCTTGCATCCAAACCGACTTG
FgCdp6	OMF 2980	GCCTCTAGATGGCTCCTGCGCGTCAACAAC
	OMF 2981	CCTCCGCCTCCGCCTCCGCCGCCTCCGCCGAAGCTGCGAGCCTTGTCGATG
FgCdp8	OMF 3054	GAGGTGAGCAGTAACAAAGCG
	OMF 3056	CCTCCGCCTCCGCCTCCGCCGCCTCCGCCATTCTTGTTCCAGGCCTTCCATG
FgCdp9	OMF 3059	ACATTCGAGCTATAGACATGG
	OMF 3061	CCTCCGCCTCCGCCTCCGCCGCCTCCGCCATCCTCATCAGCGCGGGCCTTC
FgChd3	OMF 3034	CGAAACCAAAGCCGATGACGGG
	OMF 3035	CCTCCGCCTCCGCCTCCGCCGCCTCCGCCTGTATGCTGTACTGCGCTCTC

Table 5: Primers used to construct GFP-S tag-*hph*$^{+}$ fusion cassettes

Gene Candidate	Fragment	Primer	Gene Candidate	Fragment	Primer
FgCdp1	5’ Flank	OMF 2961	*FgCdp6*	5’ Flank	OMF 2980
		OMF 3228			OMF 3228
	3’ Flank	OMF 3227		3’ Flank	OMF 3227
		OMF 2964			OMF 2983
FgCdp2	5’ Flank	OMF 2970	*FgCdp8*	5’ Flank	OMF 3054
		OMF 3228			OMF 3228
	3’ Flank	OMF 3227		3’ Flank	OMF 3227
		OMF 2969			OMF 3068
FgCdp3	5’ Flank	OMF 2973	*FgCdp9*	5’ Flank	OMF 3059
		OMF 3228			OMF 3228
	3’ Flank	OMF 3227		3’ Flank	OMF 3227
		OMF 2976			OMF 3063
FgCdp5	5’ Flank	OMF 3044	*FgChd3*	5’ Flank	OMF 3034
		OMF 3228			OMF 3228
	3’ Flank	OMF 3227		3’ Flank	OMF 3227
		OMF 3048			OMF 3037

Table 6: Transformed *F. graminearum* strains verified by Southern blot

Transformation	Obtained Verified Strains	Strain(s) on Corresponding Southern Blot
ΔFgCdp1::neo	1	1
FgCdp1-GFP-S tag-hph	0	N/A
ΔFgCdp2::neo	2	5, 6
FgCdp2-GFP-S tag-hph	1	1
ΔFgCdp3::neo	1	1
FgCdp3-GFP-S tag-hph	4	1, 2, 4, 5
ΔFgCdp5::neo	1	1
ΔFgCdp6::neo	2	4, 7
FgCdp6-GFP-S tag-hph	1	2
ΔFgCdp8::neo	0	N/A
ΔFgCdp9::neo	1	2
ΔFgChd3::neo	1	1

Table 7: NuA4 and Rpd3S complex compositions in yeast, mammals, and *F. graminearum*

Complex	**NuA4**			**Rpd3S**		
	Yeast	Mammals	*F. graminearum*	Yeast	Mammals	*F. graminearum*
Complex Subunits	Tra1	TRRAP	FGSG_06089	Rpd3	HDAC1, HDAC2	RPD3 (FGSG_01353.3)
	Eaf1	p400	FGSG_05512	Ume1	RbAp46, RbAp48	Unknown
	Epl1	EPC1	FGSG_07405	Sin3	Sin3A	FGSG_09306
	Eaf3	MRG15	FGSG_14036	Eaf3	MRG15	FGSG_14036
	Esa1	Tip60/Tip60b	HatE (FGSG_04254.3)	Rco1	N/A	FGSG_13027.3
	Eaf2	DMAP1	SWR1-complex protein 4 (FGSG_10068.3)			
	Yng2	ING1-5	FGSG_01354.3			
	Arp4	BAF53a	FGSG_00874			
	Act1	Actin	Actin (FGSG_07335.3)			
	Yaf9	GAS41	FGSG_06737			
	Eaf5	Unknown	Unknown			
	Eaf7	MRGBP	FGSG_10529			
	Eaf6	hEaf6	Unknown			

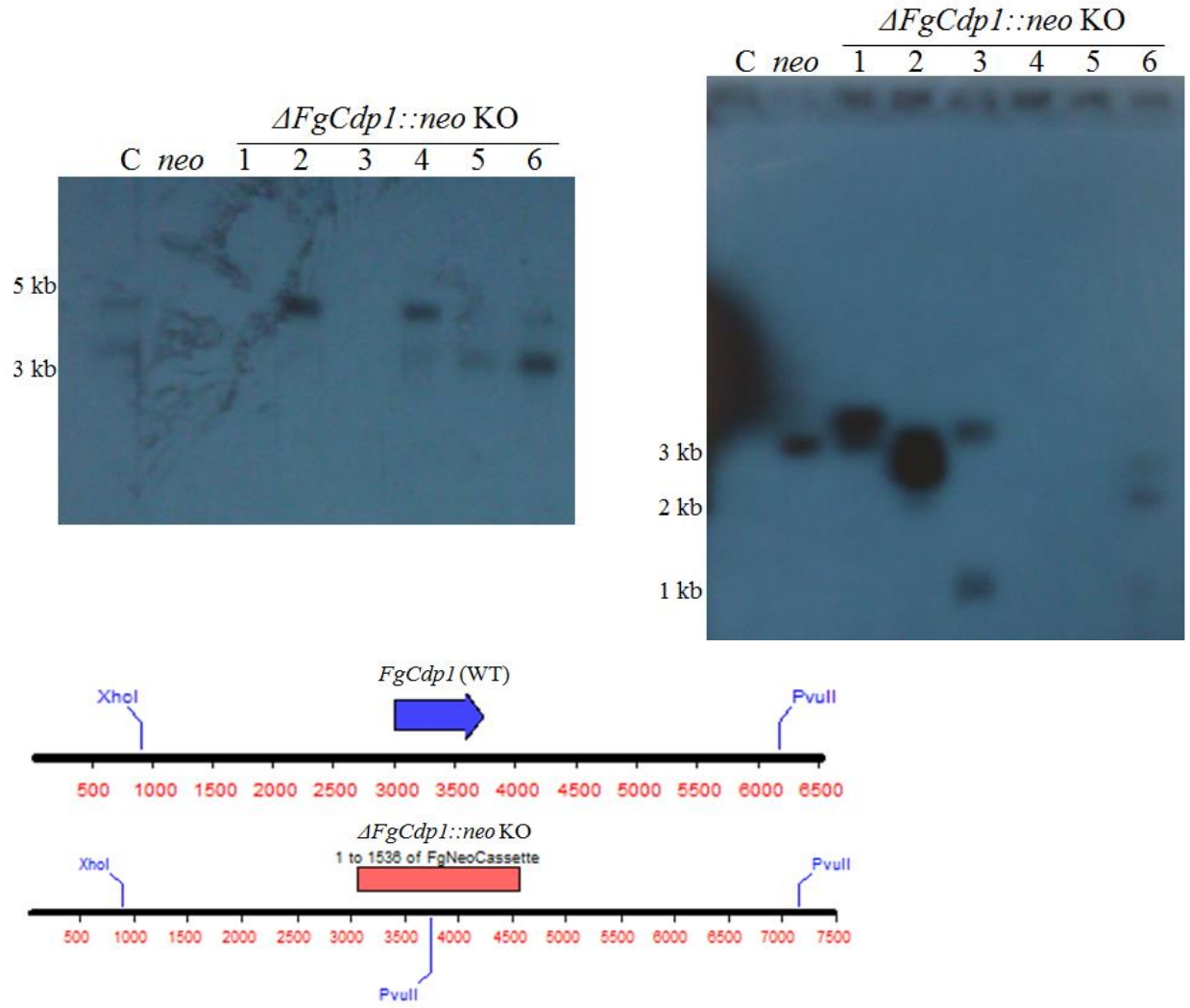

Figure 1: Southern blot for *ΔFgCdp1::neo* deletion strain, probed with either the *FgCdp1* gene (left) or the *neo*$^{+}$ gene (right). C is a wildtype control, and *neo*/*hph* are antibiotic probe positive controls. Lanes 1-6 are transformant strains. Restriction enzyme cut maps are shown below.

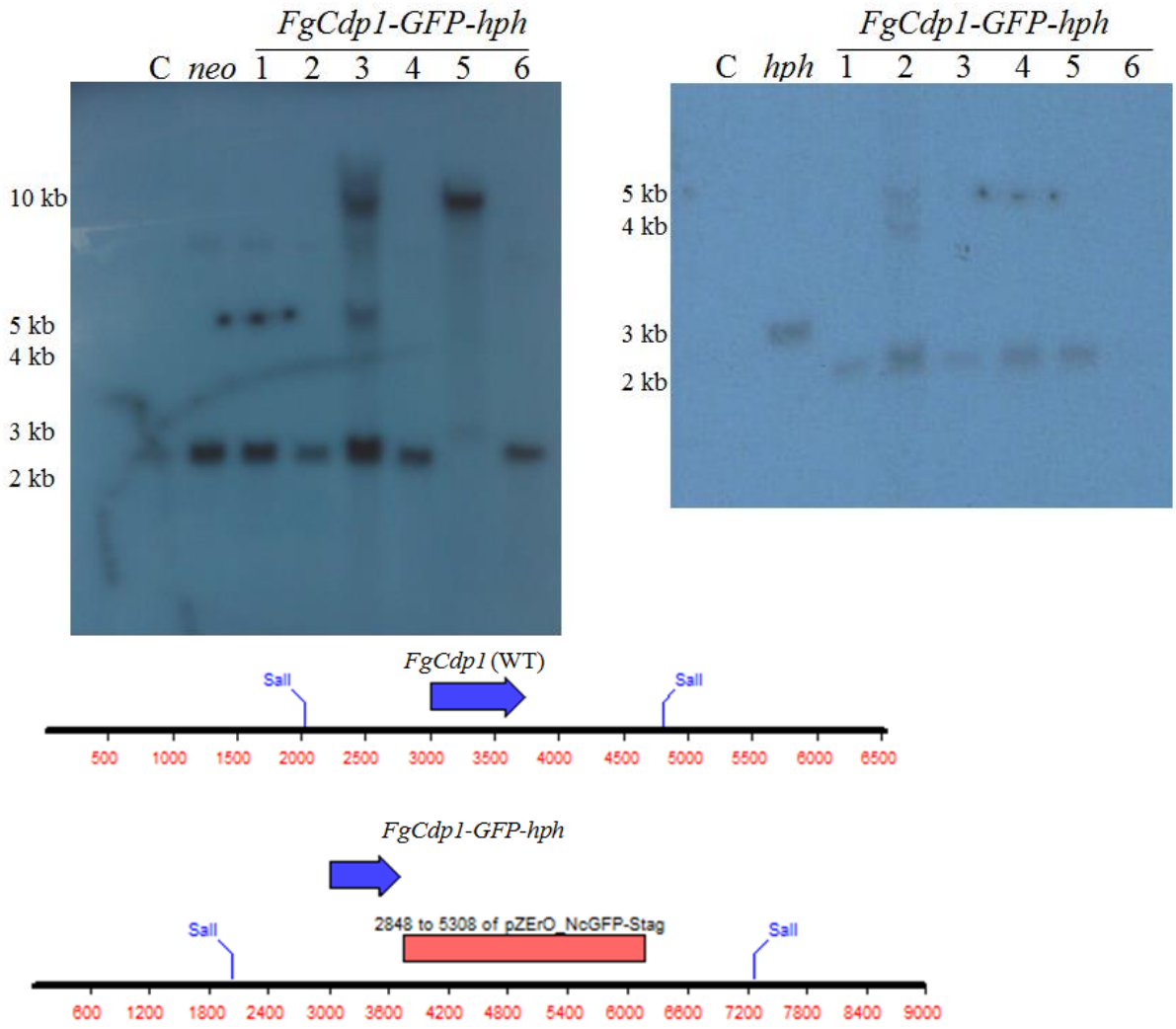

Figure 2: Southern blot results for *FgCdp1-GFP-S tag-hph*$^{+}$ transformant strains, probed with the *FgCdp1* gene. C is a wildtype control, and *neo*/*hph* are antibiotic probe positive controls. Lanes 1-6 are transformant strains. Gene probe results are on the left and *hph*$^{+}$ results on the right. Restriction enzyme cut maps are shown below.

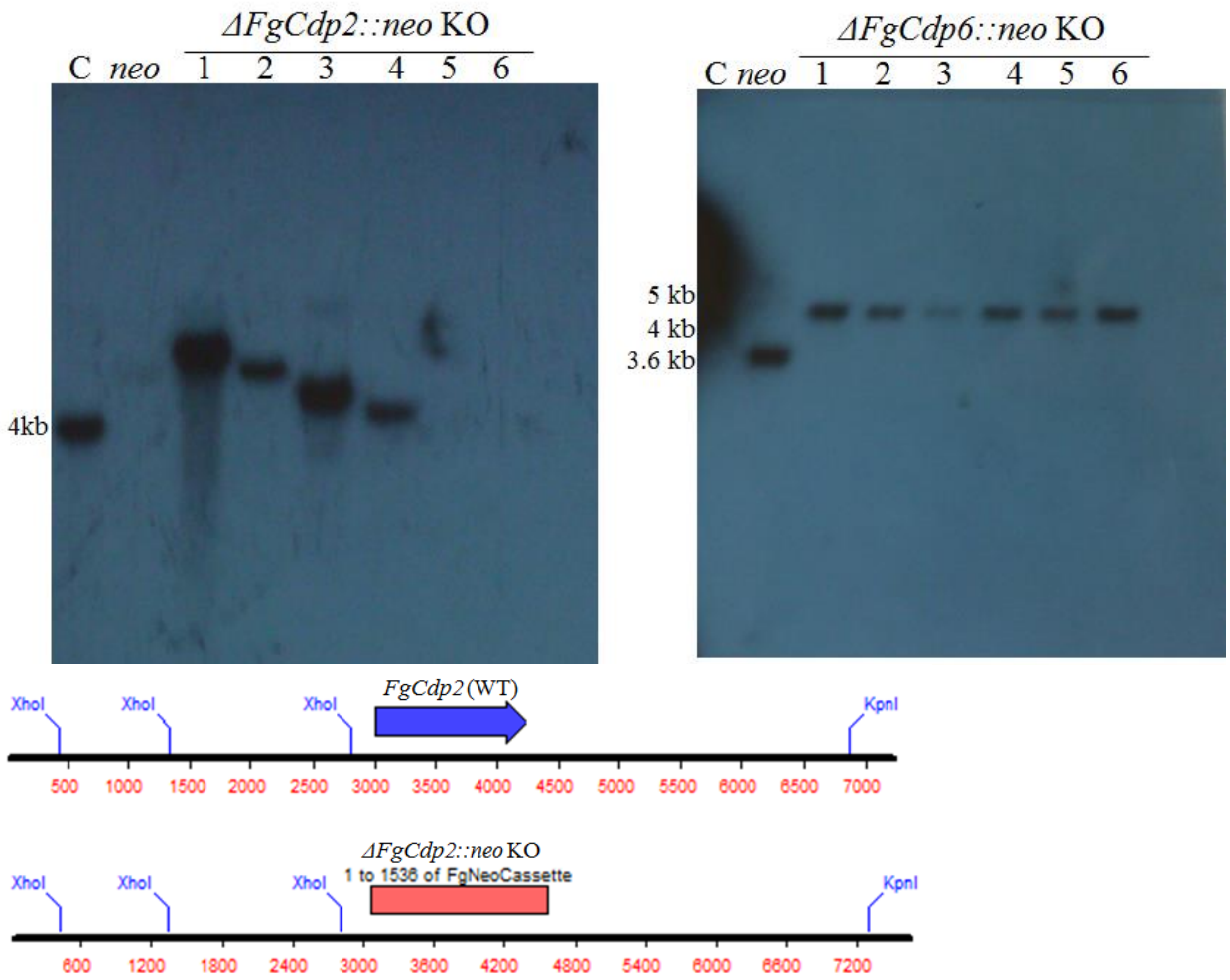

Figure 3: Southern blots for *ΔFgCdp2::neo* deletion strains, probed with either the *FgCdp2* gene (left) or the *neo*$^{+}$ gene (right). C is a wildtype control, and *neo*/*hph* are antibiotic probe positive controls. Lanes 1-6 are transformant strains. Restriction enzyme cut maps are shown as well.

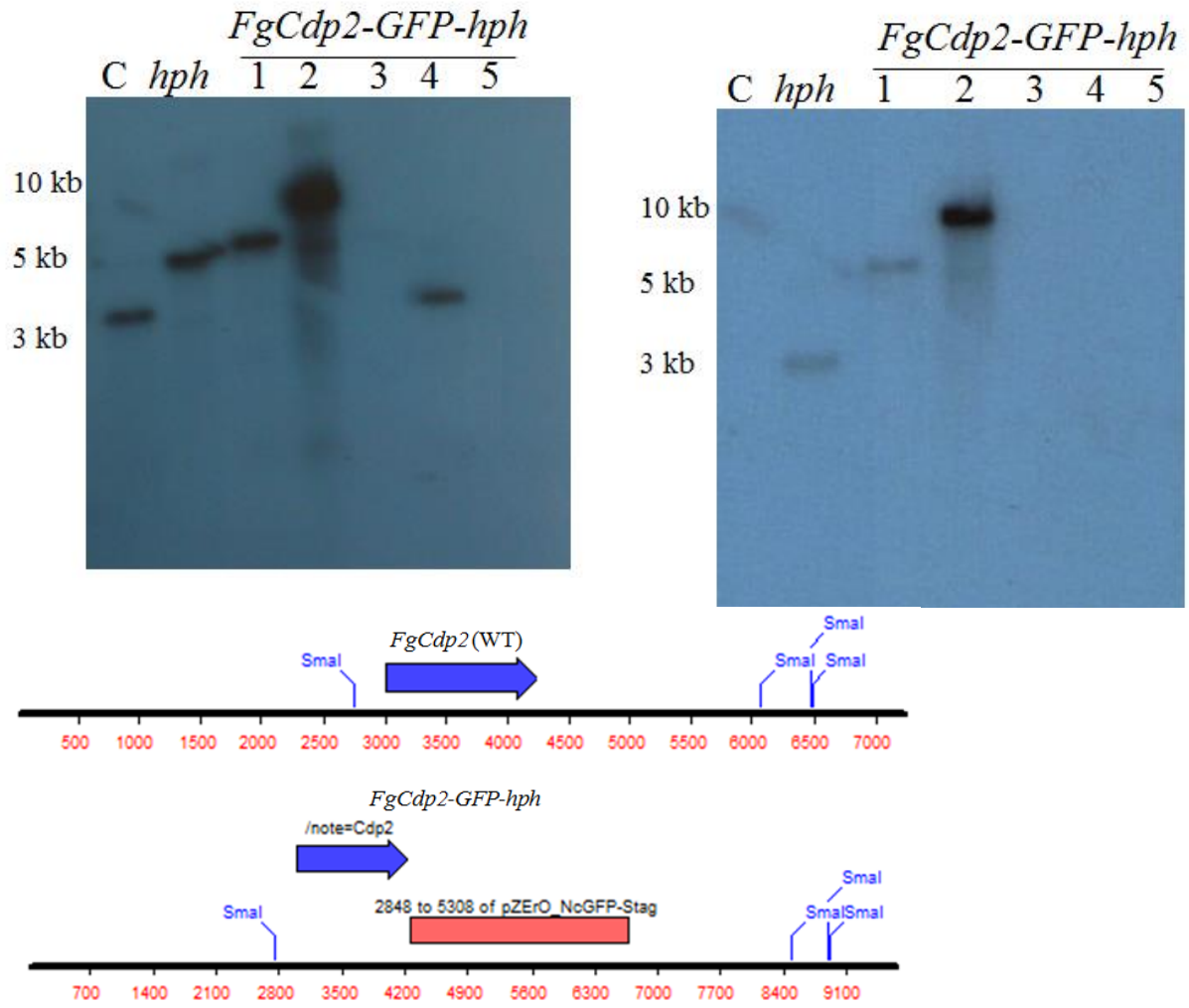

Figure 4: Southern blot results for *FgCdp2-GFP-S tag-hph*$^{+}$ strains. C is a wildtype control, and *neo*/*hph* are antibiotic probe positive controls. Lanes 1-5 are transformant strains. Gene probe results are on the left and *hph*$^{+}$ results on the right. Restriction enzyme cut maps are shown as well.

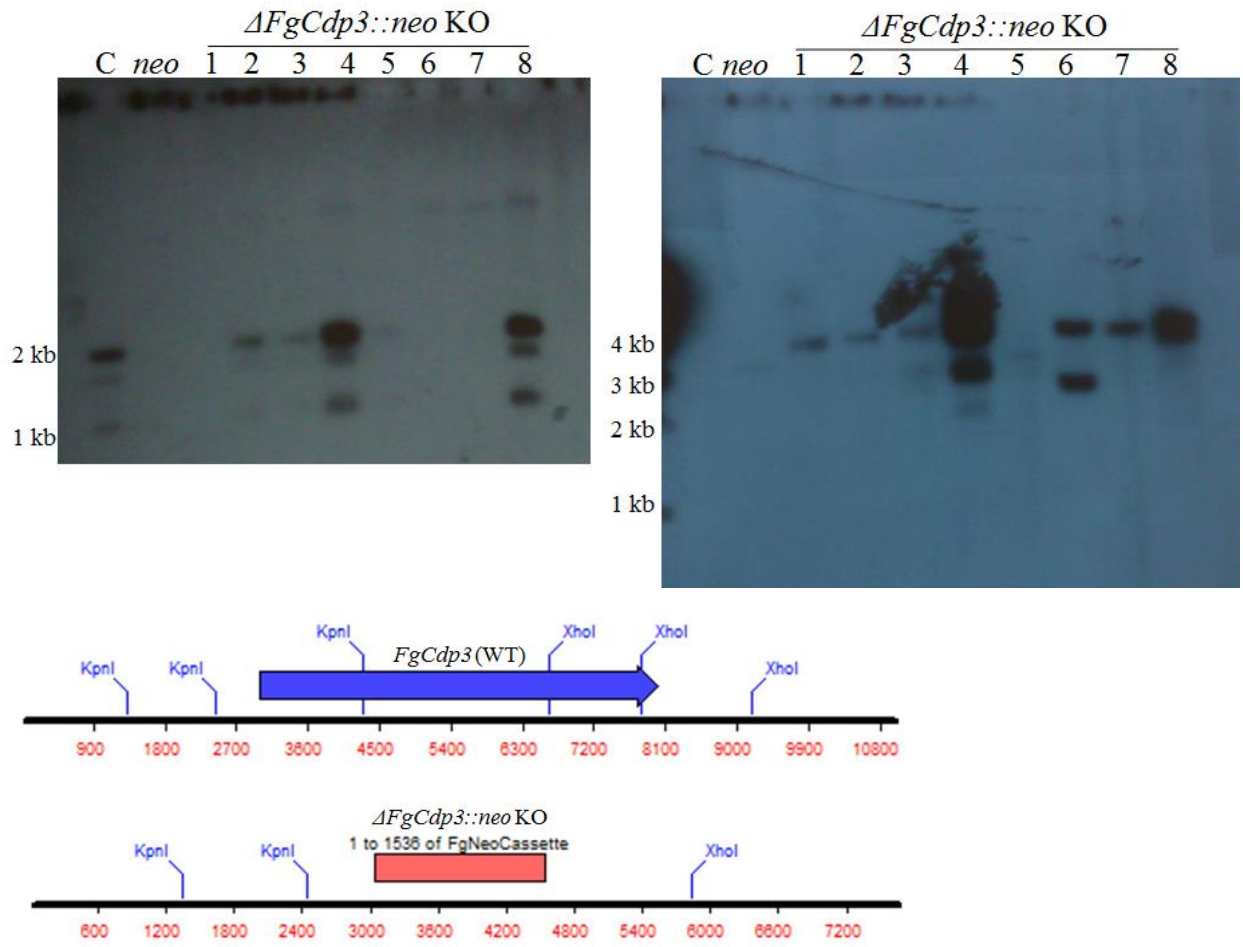

Figure 5: Southern blots for *ΔFgCdp3::neo* deletion strains, probed with either the *FgCdp3* gene (left) or the *neo*$^{+}$ gene (right). C is a wildtype control, and *neo*/*hph* are antibiotic probe positive controls. Lanes 1-8 are transformant strains. Restriction enzyme cut maps are shown as well.

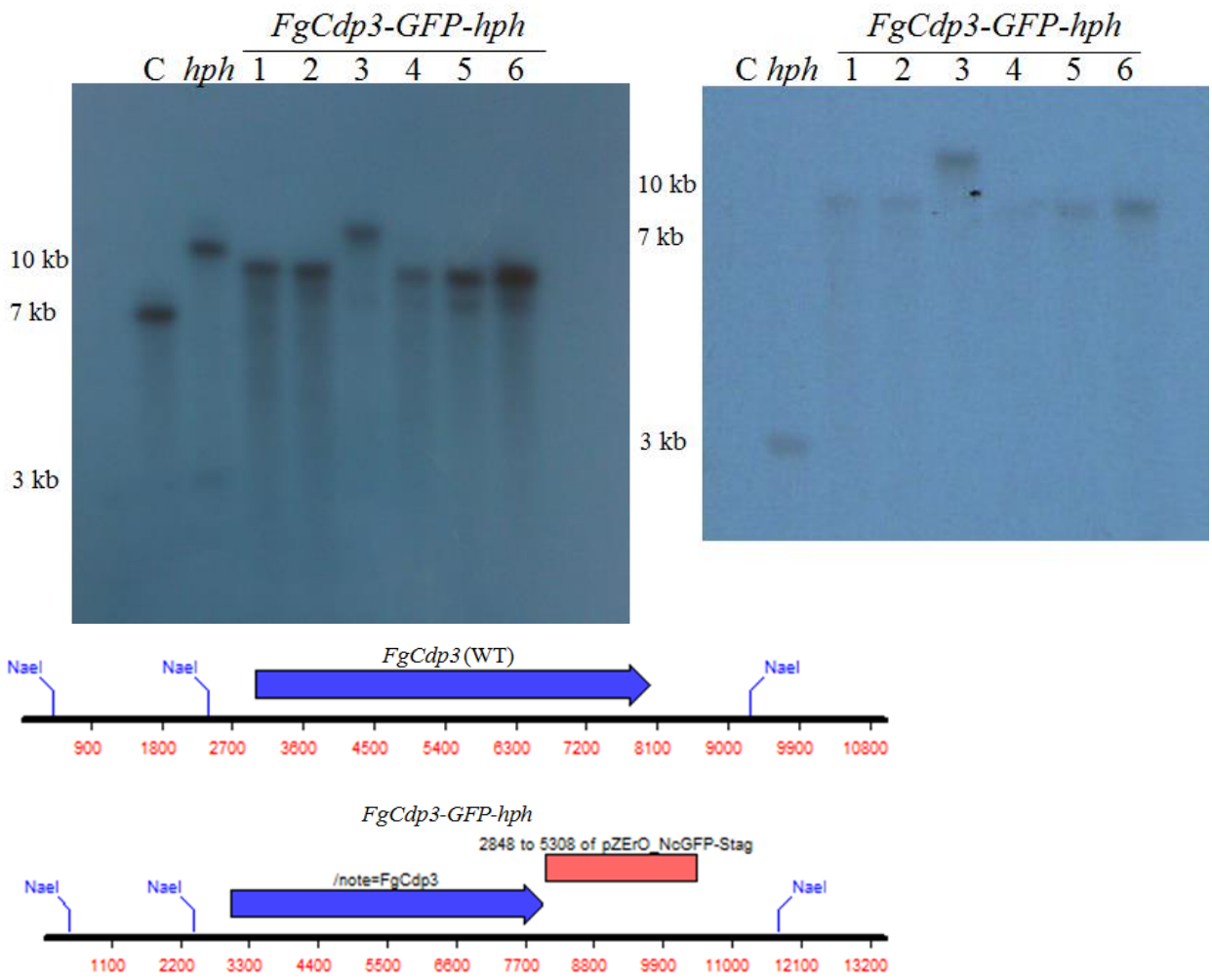

Figure 6: Southern blot results for *FgCdp3-GFP-S tag-hph*$^{+}$ strains. C is a wildtype control, and *neo*/*hph* are antibiotic probe positive controls. Lanes 1-6 are transformant strains. Gene probe results are on the left and *hph*$^{+}$ results on the right. Restriction enzyme cut maps are shown as well.

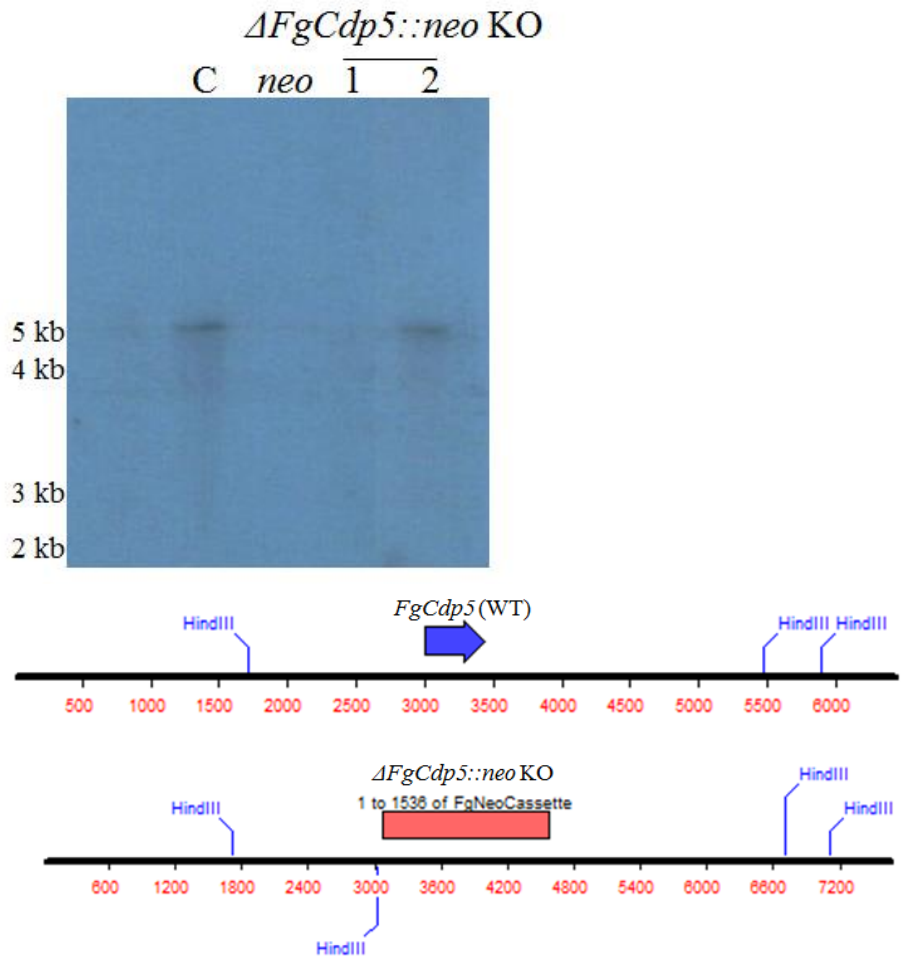

Figure 7: *ΔFgCdp5::neo* deletion Southern blot results using the *FgCdp5* gene as a probe. C is a wildtype control, and *neo*/*hph* are antibiotic probe positive controls. Lanes 1 and 2 are transformant strains. Restriction enzyme cut maps are shown as well.

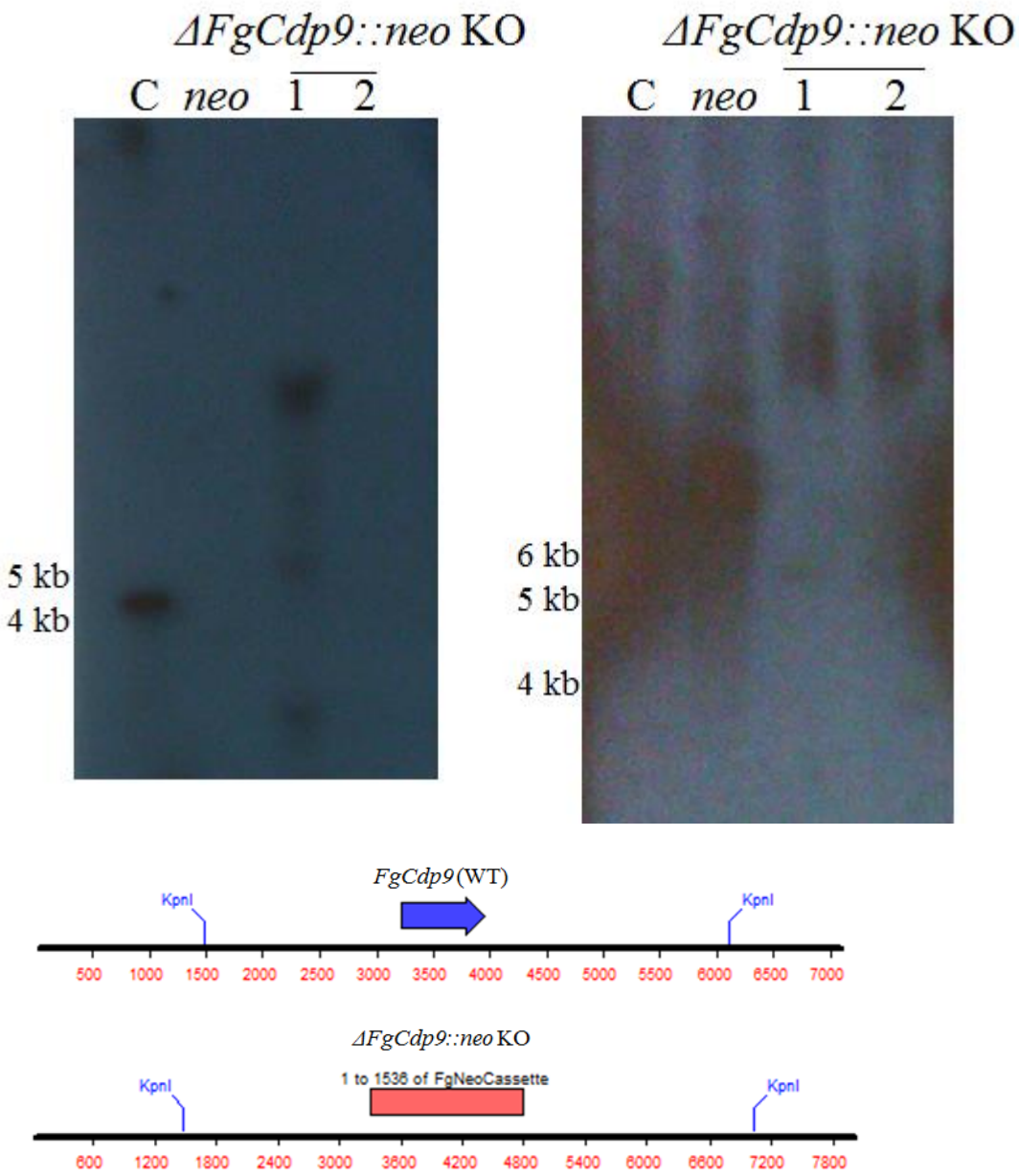

Figure 8: *ΔFgCdp9::neo* Southern blot results using either the *FgCdp9* gene (left) or *neo*$^{+}$ gene (right). C is a wildtype control, and *neo*/*hph* are antibiotic probe positive controls. Lanes 1 and 2 are transformant strains. Restriction enzyme cut maps are shown as well.

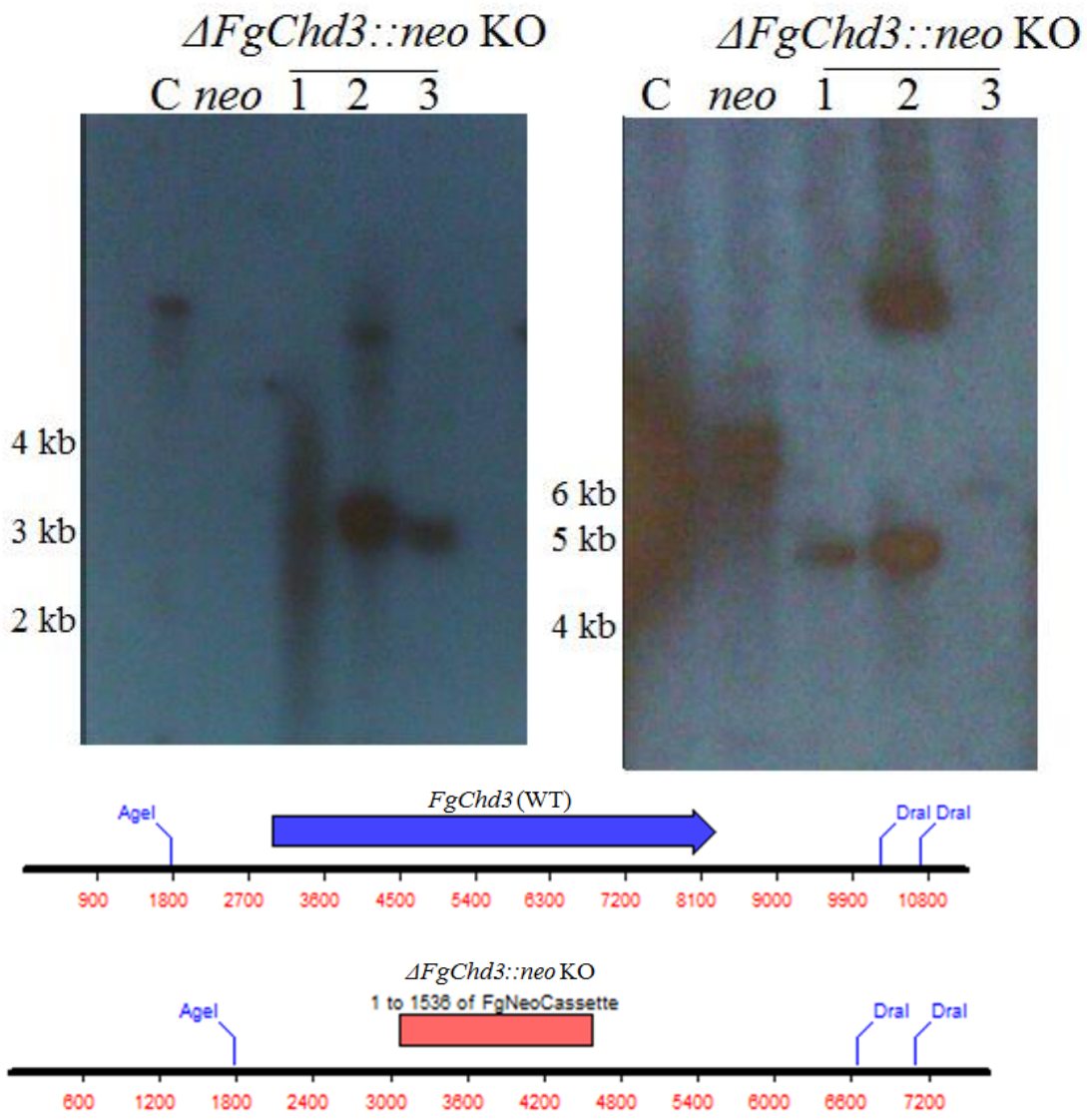

Figure 9: *ΔFgChd3::neo* Southern blot results using either the *FgChd3* gene (left) or *neo*$^{+}$ gene (right). C is a wildtype control, and *neo*/*hph* are antibiotic probe positive controls. Lanes 1, 2, and 3 are transformant strains. Restriction enzyme cut maps are shown as well.

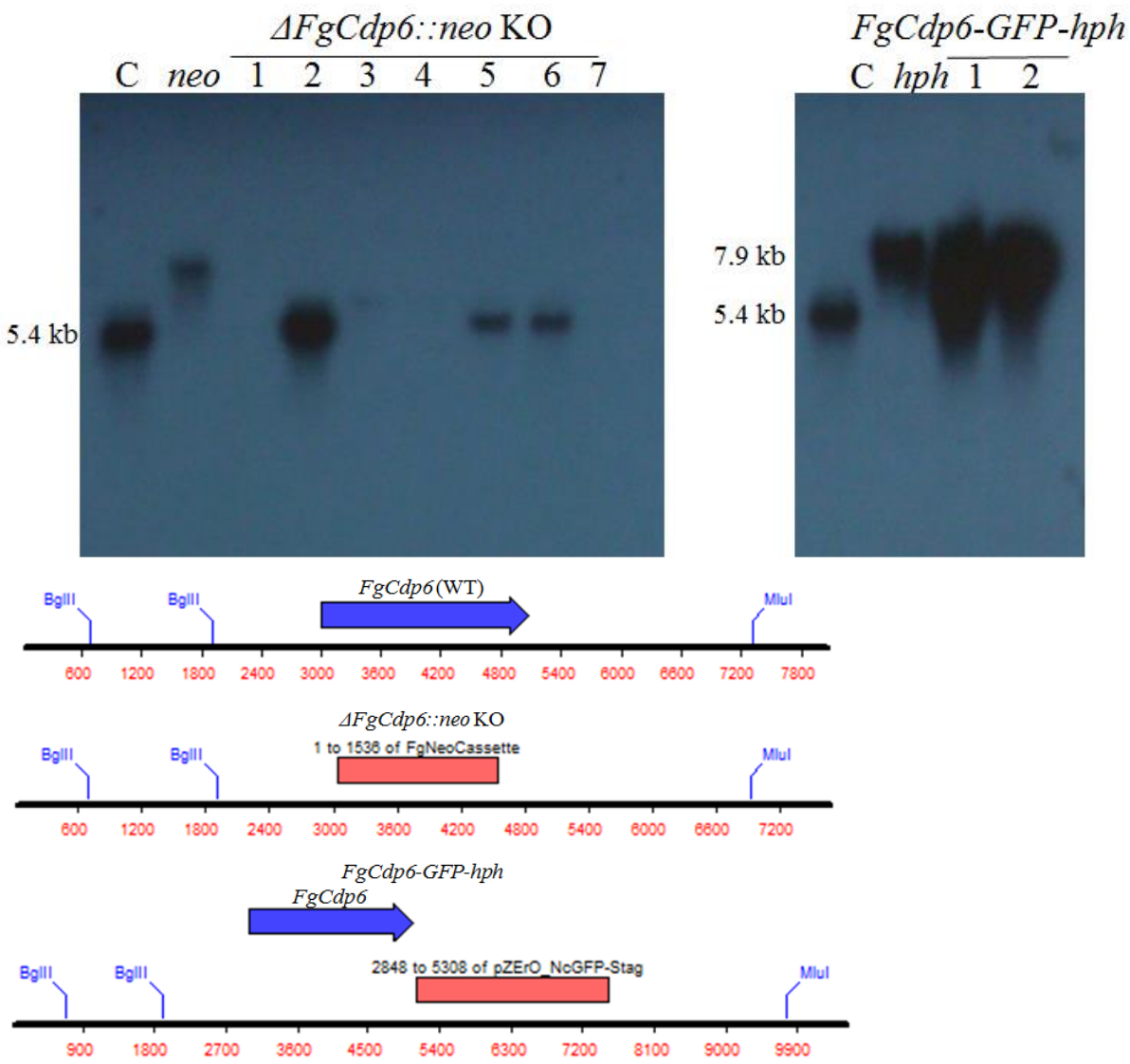

Figure 10: Southern blot results for *ΔFgCdp6::neo* deletion strains (left) as well as *FgCdp6-GFP-S tag-hph*$^{+}$ fusion strains (right) when probing with the *FgCdp6* gene. C is a wildtype control, and *neo*/*hph* are antibiotic probe positive controls. Numbered lanes are different transformant strains being verified. Restriction enzyme cut maps are shown as well.

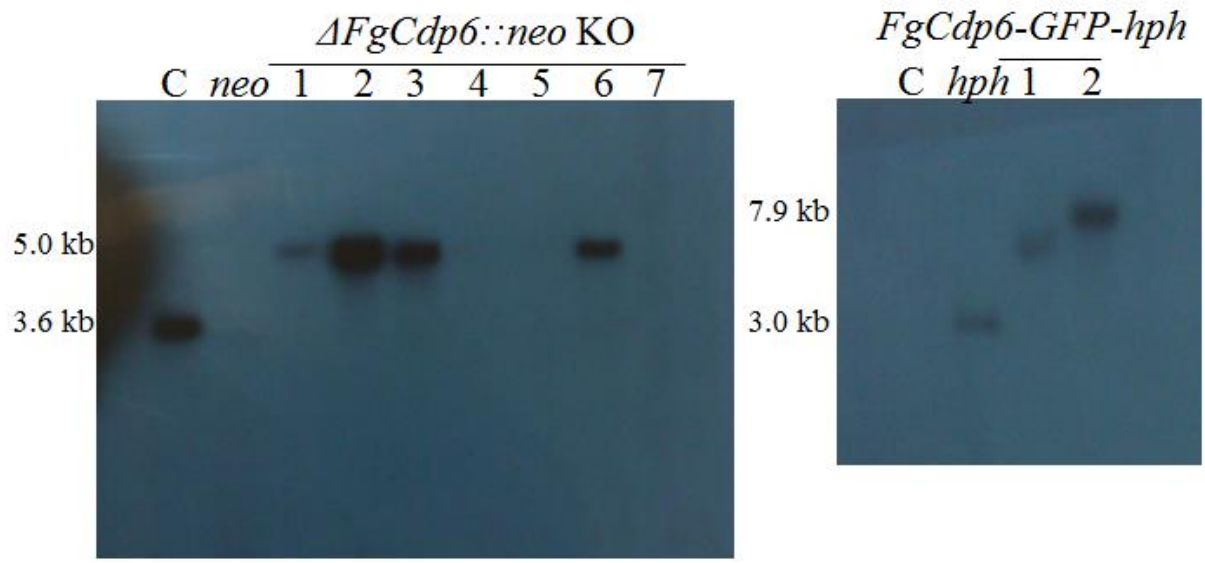

Figure 11: Southern blot results for *ΔFgCdp6::neo* deletion strains (left) as well as *FgCdp6-GFP-S tag-hph*$^{+}$ fusion strains (right) when probing with antibiotic genes (*neo*$^{+}$ for deletion strains and *hph*$^{+}$ for fusion strains). C is a wildtype control, and *neo*/*hph* are antibiotic probe positive controls. Numbered lanes are different transformant strains being verified. Restriction enzyme cut maps are shown in Figure 10.

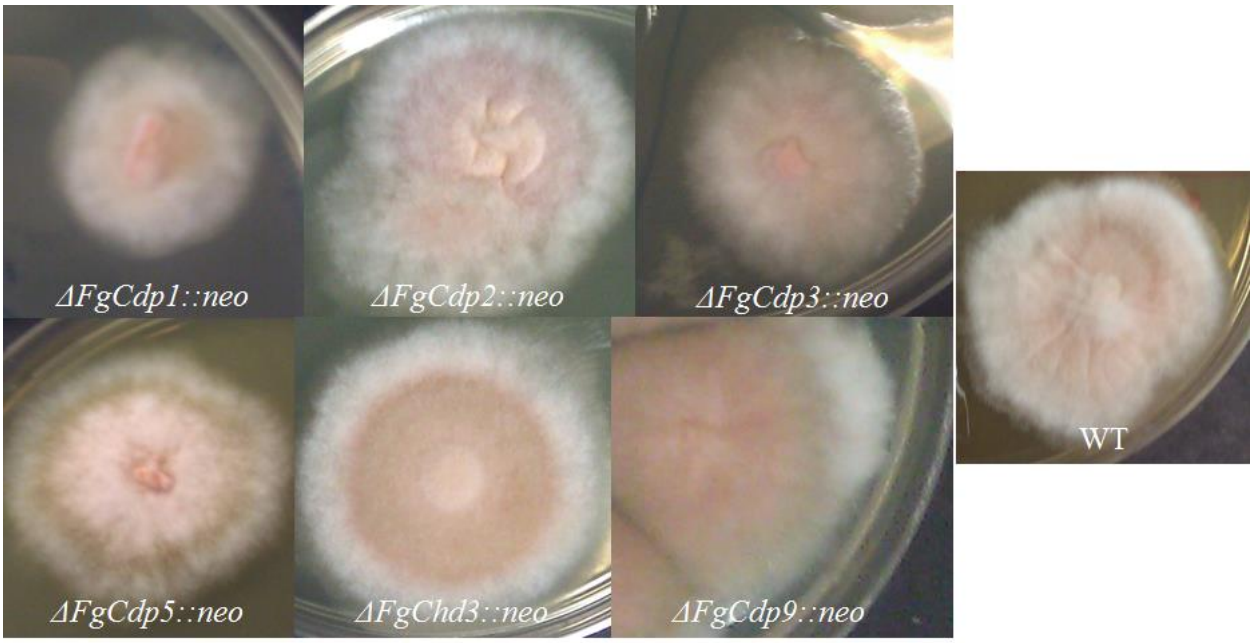

Figure 12: Targeted genetic knockouts for six genes; all of them have phenotypes similar to the wild type. All fungi in this picture were grown for about three days on YPD agar. Differences in colonies, in both growth and appearance, can be attributed to difference in inoculum type (either asexual spores or mycelia on agar) and size.

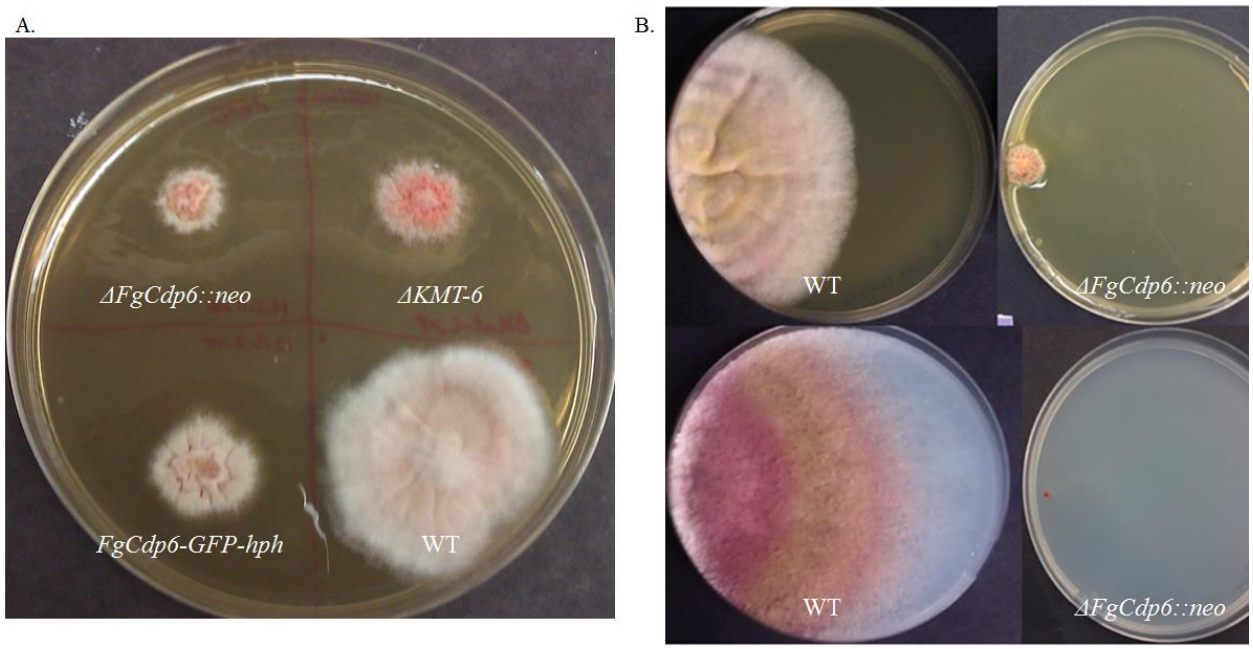

Figure 13: A. Phenotypic differences between wildtype *F. graminearum* and *FgCdp6* strains (top left is a *ΔFgCdp6::neo* knockout strain, top right is the *ΔKmt-6* mutant known for a specific phenotype in *F. graminearum*, bottom right is WT, and bottom left is a *FgCdp6-GFP-S tag-hph*$^{+}$ fusion strain). B. Differences in growth between PH-1 and *ΔFgCdp6::neo* on both YPD (top two pictures) and FMM (bottom two pictures). In both cases, the left photo is of wildtype PH-1 and the right photo is the *ΔFgCdp6::neo* strain. All four plates were inoculated with a single spore and were allowed to grow for seven days.

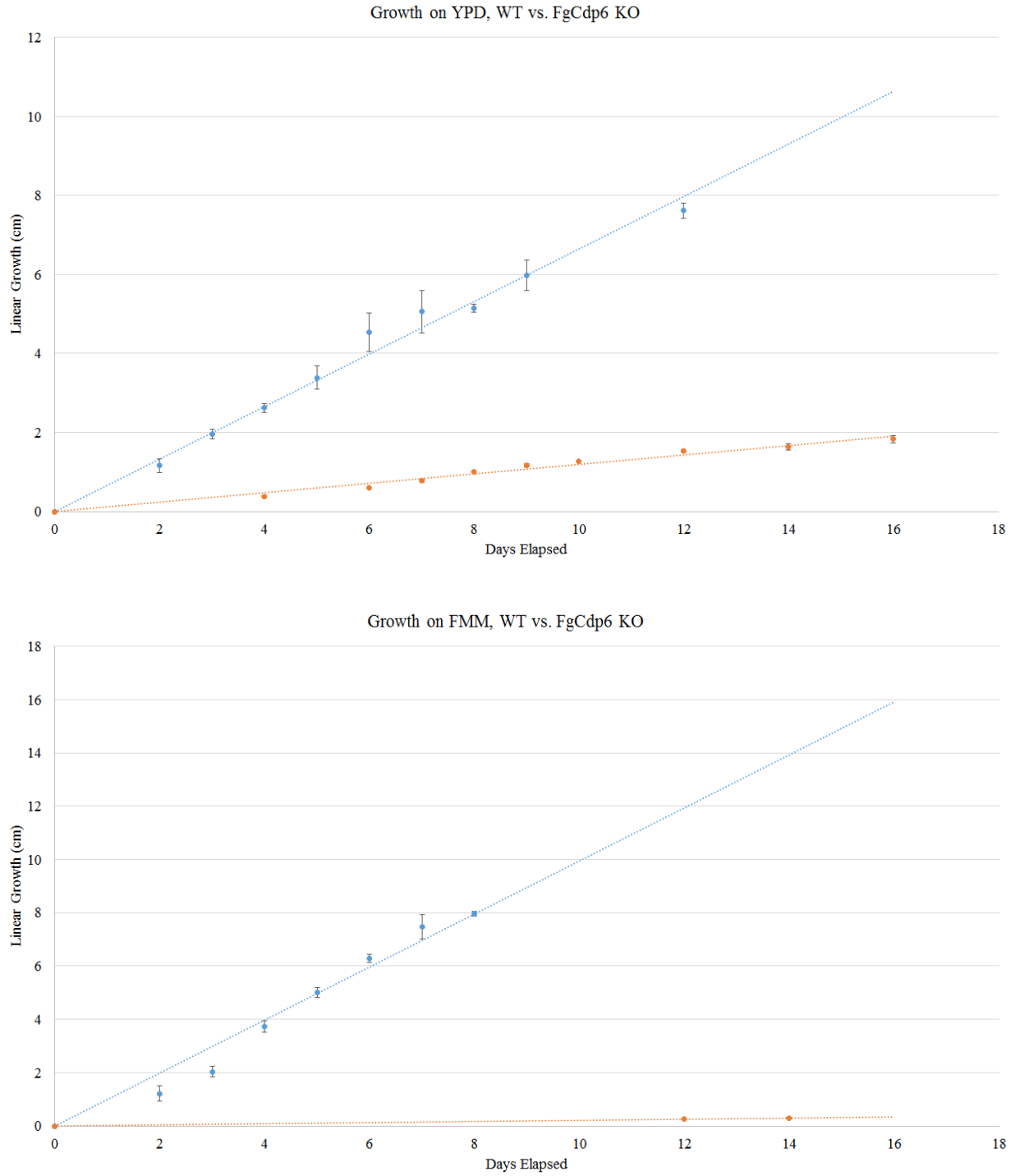

Figure 14: Linear growth differences between wildtype *F. graminearum* (blue) and a verified *ΔFgCdp6::neo* knockout strain (orange). Assays were conducted on either YPD agar (above) or FMM agar (below). On YPD agar, the wildtype fungus grew at a rate of 0.66cm/day (R^2=0.9868), while the deletion strain grew by 0.12cm/day (R^2=0.9804). On FMM agar, the wildtype fungus grew by 1.00cm/day (R^2=0.9687), and the deletion strain grew by 0.02cm/day (R^2=0.9985). Error bars display standard deviation between replicate plates (points without visible error bars have little to no deviation).

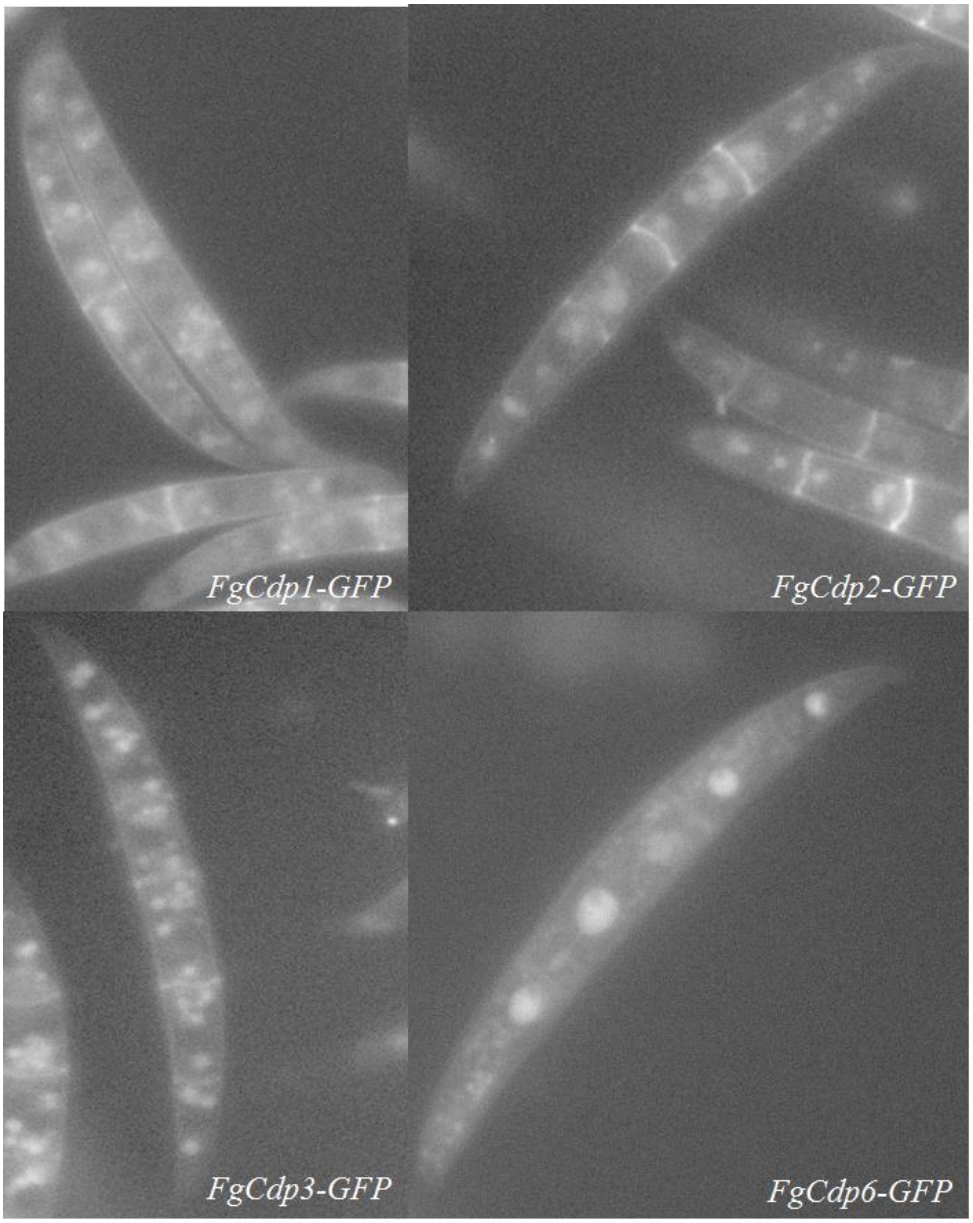

Figure 15: GFP localization in tagged strains. Localization is only observed in the *FgCdp6* strain, the other three strains either had very little or no fluorescence resulting in a high amount of backround.

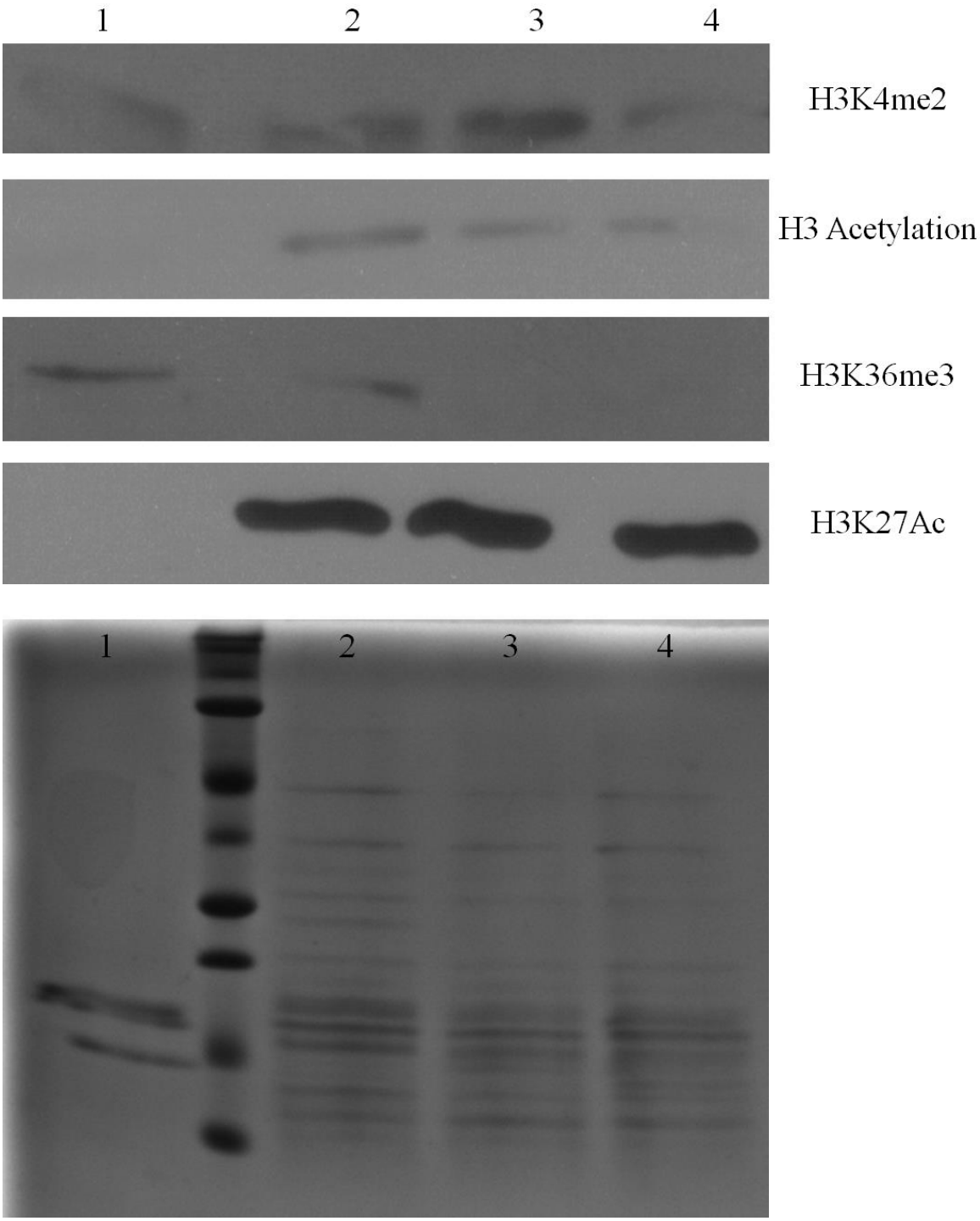

Figure 16: Western blot results using four different primary antibodies (on the right). Lane 1 is a control or calf thymus histones, lane 2 histones from wildtype PH-1, lane 3 *FgCdp6* deletion strain histones, and lane 4 *FgCdp6-GFP-S tag* fusion strain histones. A Coomassie Blue stained gel is also present (below) to observe relative amounts of histones in each lane.

Bibliography

1. Wheatley, R. W., Lo, S., Jancewicz, L. J., Dugdale, M. L., & Huber, R. E. (2013). Structural explanation for allolactose (lac operon inducer) synthesis by lacZ β-galactosidase and the evolutionary relationship between allolactose synthesis and the lac repressor. *The Journal of biological chemistry*, *288*(18), 12993–3005. doi:10.1074/jbc.M113.455436

2. De Santa, F., Totaro, M. G., Prosperini, E., Notarbartolo, S., Testa, G., & Natoli, G. (2007). The histone H3 lysine-27 demethylase Jmjd3 links inflammation to inhibition of polycomb-mediated gene silencing. *Cell*, *130*(6), 1083–94. doi:10.1016/j.cell.2007.08.019

3. Thoma, F., Koller, T., & Klug, a. (1979). Involvement of histone H1 in the organization of the nucleosome and of the salt-dependent superstructures of chromatin. *The Journal of cell biology*, *83*(2 Pt 1), 403–27.

4. Du Toit, A. (2012). Chromatin: Defining heterochromatin. *Nature reviews. Molecular cell biology*, *13*(11), 684–5. doi:10.1038/nrm3450

5. Chen, L., & Widom, J. (2004). Molecular basis of transcriptional silencing in budding yeast. *Biochemistry and Cell Biology*, *418*, 413–418. doi:10.1139/O04-035

6. Boros, I. M. (2012). Histone modification in Drosophila. *Briefings in functional genomics*, *11*(4), 319–31. doi:10.1093/bfgp/els029

7. Lauberth, S. M., Nakayama, T., Wu, X., Ferris, A. L., Tang, Z., Hughes, S. H., & Roeder, R. G. (2013). H3K4me3 interactions with TAF3 regulate preinitiation complex assembly and selective gene activation. *Cell*, *152*(5), 1021–36. doi:10.1016/j.cell.2013.01.052

8. Connolly, LR, Smith KM, Freitag, M (2013) "The *Fusarium graminearum* Histone H3 K27 Methyltransferase KMT6 Regulates Development and Expression of Secondary Metabolite Gene Clusters" PLoS Genet 9(10): e1003916. doi:10.1371/journal.pgen.1003916

9. Jones, D. O., Cowell, I. G., & Singh, P. B. (2000). Mammalian chromodomain proteins: their role in genome organisation and expression. *BioEssays : news and reviews in molecular, cellular and developmental biology*, *22*(2), 124–37. doi:10.1002/(SICI)1521-1878(200002)22:2<124::AID-BIES4>3.0.CO;2-E

10. Simon, J. a, & Kingston, R. E. (2009). Mechanisms of polycomb gene silencing: knowns and unknowns. *Nature reviews. Molecular cell biology*, *10*(10), 697–708. doi:10.1038/nrm2763

11. Honda, S., Lewis, Z. a, Shimada, K., Fischle, W., Sack, R., & Selker, E. U. (2012). Heterochromatin protein 1 forms distinct complexes to direct histone deacetylation and DNA methylation. *Nature structural & molecular biology*, *19*(5), 471–7, S1. doi:10.1038/nsmb.2274

12. Doyon, Y., Selleck, W., Lane, W. S., Tan, S., Côté, J. (2004). Structural and Functional Conservation of the NuA4 Histone Acetyltransferase Complex from Yeast to Humans. *Molecular and cellular biology*, 24(5), 1884-1896. doi:10.1128/MCB.24.5.1884

13. Bugga, L., McDaniel, I. E., Engie, L., & Armstrong, J. a. (2013). The Drosophila melanogaster CHD1 chromatin remodeling factor modulates global chromosome structure and counteracts HP1a and H3K9me2. *PloS one*, *8*(3), e59496. doi:10.1371/journal.pone.0059496

14. Chen, M., Tominaga, K., & Pereira-Smith, O. M. (2010). The Emerging Role of the MORF/MRG Gene Family in Various Biological Processes Including Aging. *Annals of the NY Academy of Sciences*, *1197*, 134–141. doi:10.1111/j.1749-6632.2010.05197.

15. Terpe, K. (2003). Overview of tag protein fusions: from molecular and biochemical fundamentals to commercial systems. *Applied microbiology and biotechnology*, *60*(5), 523–33. doi:10.1007/s00253-002-1158-6

16. Gilbert, J., & Haber, S. (2013). Overview of some recent research developments in fusarium head blight of wheat. *Canadian Journal of Plant Pathology*, *35*(2), 149–174. doi:10.1080/07060661.2013.772921

17. Daniel G. Gibson, Chapter fifteen - Enzymatic Assembly of Overlapping DNA Fragments, In: Christopher Voigt, Editor(s), Methods in Enzymology, Academic Press, 2011, Volume 498, Pages 349-361, ISSN 0076-6879, ISBN 9780123851208, http://dx.doi.org/10.1016/B978-0-12-385120-8.00015-2.

18. Pomraning, K. R., Smith, K. M., & Freitag, M. (2009). Genome-wide high throughput analysis of DNA methylation in eukaryotes. *Methods*, *47*(3), 142–150. doi:10.1016/j.ymeth.2008.09.022

19. Miao VP, Freitag M, Selker EU (2000) Short TpA-rich segments of the ζ-η region induce DNA methylation in *Neurospora crassa*. *J Mol Biol* 300: 249-273.

20. Filesi, I., Cardinale, A., van der Sar, S., Cowell, I. G., Singh, P. B., & Biocca, S. (2002). Loss of heterochromatin protein 1 (HP1) chromodomain function in mammalian cells by intracellular antibodies causes cell death. *Journal of cell science*, *115*(Pt 9), 1803–13.

21. Eisen, a, Utley, R. T., Nourani, a, Allard, S., Schmidt, P., Lane, W. S., … Cote, J. (2001). The yeast NuA4 and Drosophila MSL complexes contain homologous subunits important for transcription regulation. *The Journal of biological chemistry*, *276*(5), 3484–91. doi:10.1074/jbc.M008159200

22. Reid, J. L., Moqtaderi, Z., & Struhl, K. (2004). Eaf3 Regulates the Global Pattern of Histone Acetylation in Saccharomyces cerevisiae, *24*(2), 757–764. doi:10.1128/MCB.24.2.757

23. Doyon, Y., & Côté, J. (2004). The highly conserved and multifunctional NuA4 HAT complex. *Current opinion in genetics & development*, *14*(2), 147–54. doi:10.1016/j.gde.2004.02.009

24. Li, B., Gogol, M., Carey, M., Lee, D., Seidel, C., & Workman, J. L. (2007). Combined Action of PHD and Chromo Domains Directs the Rpd3S HDAC to Transcribed Chromatin. *Science*, *316*, 1050–1054.

25. Yang, X.-J., & Seto, E. (2008). The Rpd3/Hda1 family of lysine deacetylases: from bacteria and yeast to mice and men. *Nature reviews. Molecular cell biology*, *9*(3), 206–18. doi:10.1038/nrm2346